Chapter 1

CHAPTER 1: Peek into world of next generation Wonder material - Graphene

In this chapter we first briefly introduce carbon and its allotropes followed by a general introduction to essential features and properties of Graphene. Few techniques of obtaining graphene experimentally have been presented. Density-Density response function that has been used for investigations reported in forthcoming chapters, is briefly reviewed along with discussion on dynamic dielectric function by citing important references. A brief review of many particle aspects and collective excitations of graphene and graphene based systems have been reported. The various aspects including structure factor, pair distribution function, screening charge density, self energy, compressibility, energy loss, wake effects, plasmon-phonon coupled modes of various graphene based systems are introduced in this chapter. Our motivation to perform the work has been mentioned at the end followed by listing the references, which have been cited throughout the chapter.

1.1 Background

1.1.1 Carbon and its allotropes

Carbon being the prominent and quite easily available element is considered as the chemical basis of all known life. It has the affinity for bonding with other small atoms and is capable of forming stable covalent bonds with such atoms and hence can be considered as building blocks of nanomaterial. Carbon has four valence electrons which hybridize with other electrons of neighbouring atoms giving rise to different allotropes. There has been extensive investigation on different allotropes of carbon for years, including graphite, diamond, carbon nanotubes and fullerene.

1.1.1.1. Graphite

Graphite is the simplest form of carbon found in nature and is considered as a good conductor. It is made up of several layers stacked one above another Fig 1.1a), with each layer comprising of carbon atoms arranged in hexagonal pattern, where each carbon atom forms 3 covalent σ-bonds resulting into a sp^2 hybridization. The remaining p-orbitals, which are perpendicular to the plane of the σ-bonds, overlap to form a delocalized π-system. The planes are widely separated as they are held together only by the weak van der Waals forces, such that these layers can slide over one another.

1.1.1.2. Diamond

A diamond is a transparent crystal of tetrahedral bonded carbon atoms in a covalent network lattice (sp^3) that crystallizes into diamond lattice. Diamond, an insulator, is strong and hard in nature because of its extreme rigid lattice structure. Moreover it has high thermal conductivity, a large band gap and high optical dispersion. It is less stable than graphite, where the carbon atoms are arranged in a variation of face centred cubic crystal structure. Because of this lattice structure there is a less possibility of diamond getting contaminated. It has billions of carbon atoms forming hexagonal structure extending in all directions Fig 1.1b).

1.1.1.3. Carbon Nanotubes

Carbon nanotubes (CNTs) are allotrpes of carbon with cylindrical nanostructure, where one atom thick sheet of carbon is rolled at specific and discrete angle to form hollow cylindrical tubes Figure 1.1c). There has been tremendous research work carried out on the CNTs because of their unique transport and optical properties. electronically these tubes behave as a metal and semiconductors.

1.1.1.4. Fullerene

Fullerene molecule contains pentagonal and hexagonal rings in which no two pentagons share an edge. It has a shape similar to that of a football and hence is famously known as bucky ball Fig 1.1d). It is also the most common in terms of natural occurrence, as it can often be found in soot. The bonds are sp^2 hybridized. Chemically it is stable but not totally unreactive.

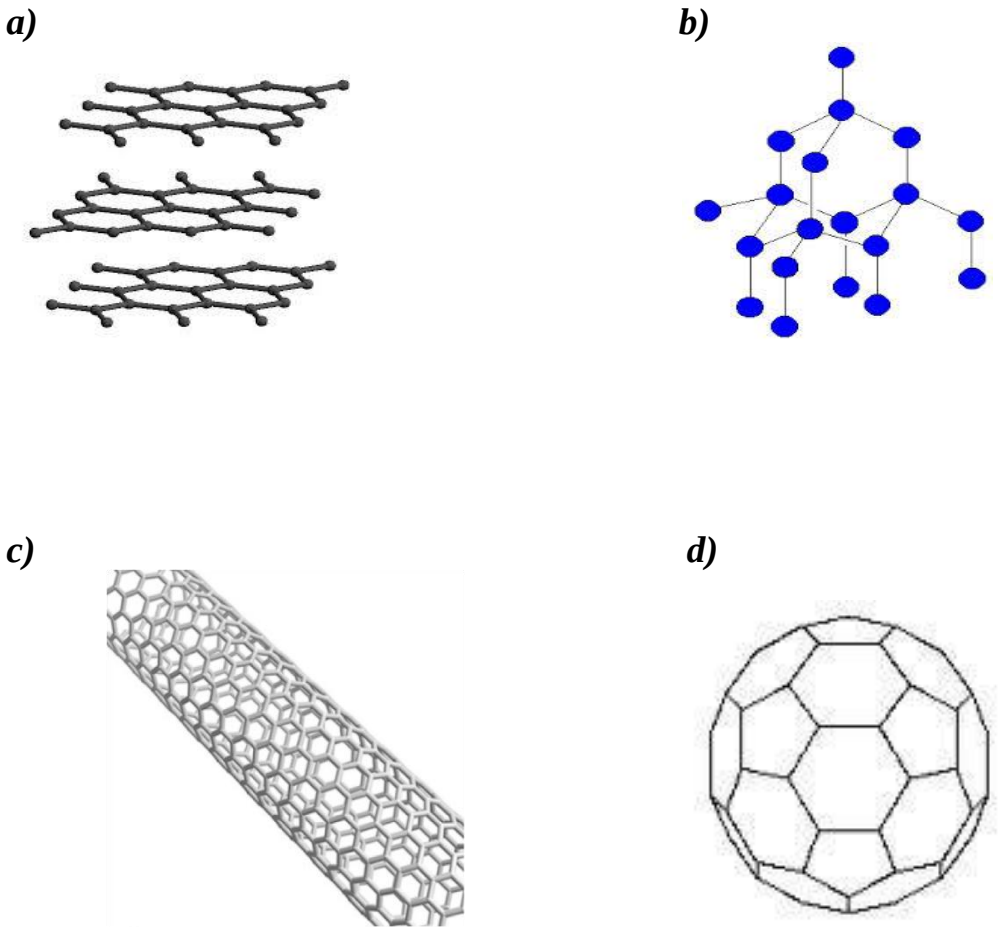

Figure 1.1 Displays allotropes of Carbon ***a)*** Graphite ***b)*** Diamond ***c)*** Carbon nanotubes ***d)*** Buckyball- Fullerene

1.1.2 Graphene

The basis of all above allotropes is Graphene, a single layer of carbon atoms covalently bonded together in a free state , Fig 1.2. Carbon has four valence electrons occupying the 2s and 2p orbitals. These orbitals interact with other orbitals of neighbouring carbon atoms forming 3 covalent sp^2 bonds, called σ bonds, which are strong in nature. The electrons are localized in the plane connecting carbon atoms and are responsible for great strength and mechanical properties of graphene , Fig 1.3. The $2p_z$ orbital electrons form weak π bond normal to the plane of carbon atoms. Graphene's real-space lattice structure is a honeycomb shaped structure lying in two dimensional plane, which comprises of two interpenetrating triangular sublattices A and B , Fig 1.4, responsible for chirality in Graphene. The two inequivalent lattice sites with atoms A and B in each unit cell of the periodic lattice are displaced from each other along an edge of the hexagons by a distance of a_0 = 1.42 Å. The nearest neighbour atoms are positioned by δ_1, δ_2 and δ_3. The primitive unit cell of the Bravais lattice is a parallelogram with vectors

$$\mathbf{a_1} = \left(\frac{\sqrt{3}a}{2}, \frac{a}{2}\right), \qquad \mathbf{a_2} = \left(\frac{\sqrt{3}a}{2}, \frac{a}{-2}\right) \tag{1.1}$$

Where $a = |\mathbf{a_1}| = |\mathbf{a_2}|$

and the reciprocal space honeycomb structure has a hexagonal Brillouin zone (fig. 1.5) with wave vectors,

$$\mathbf{b_1} = \left(\frac{2\pi}{\sqrt{3}a}, \frac{2\pi}{a}\right), \qquad \mathbf{b_2} = \left(\frac{2\pi}{\sqrt{3}a}, -\frac{2\pi}{a}\right) \tag{1.2}$$

The Brillouin zone corners at the **K**-points also known as Dirac points [1]. At these so-called Dirac points , Fig.1.6 the low-energy excitations satisfy the massless Dirac

equation, and the band structure for the Dirac fermions is uniquely different from that for the Schrödinger fermions of the regular 2DEG exhibiting a linear energy dispersion $E_k = \hbar v \vec{k}$ Fig 1.7 (having an effective speed of light $v \approx 10^6\ ms^{-1}$) with the conduction and valence bands connected at the Dirac point forming a Dirac cone, where $\vec{k}$ is the wave-vector. The two dimensional (2D) or single layer graphene (SLG) is thus a rather unique chiral Dirac system. Knowledge of band structure of SLG is important to understand the basic properties of SLG as well as of the devices based on SLG. This apparently peculiar band structure of graphene is readily accounted for using a tight-binding model with nearest-neighbor hopping, where, in the respect to the momentum. SLG is a gapless semiconductor. In intrinsic SLG, the Fermi level lies at the Dirac points, but as with other semiconductors it is possible to shift the Fermi level by either doping the sample or applying an external gate voltage, which introduces 2D free carriers, electrons or holes, producing extrinsic graphene with gate-voltage-induced tunable carrier density. The Fermi momentum k_f and the Fermi energy E_f , relative to the Dirac point energy of SLG, are given by $k_f = (4\pi n / g_s g_v)^{1/2}$ and $E_f = \hbar v_f k_f$ and the corresponding density of states (DOS) is given as $\frac{(g_s g_v n)^{\frac{1}{2}}}{\sqrt{\pi}\hbar v_f}$, where n is the 2D carrier, electron or hole density, g_s and g_v are spin and valley degeneracies, respectively [2]. The interaction parameter r_s or coupling constant which gives ratio of the potential to the kinetic energy is independent of n and is constant unlike in 2DEG $r_s = \frac{e^2}{\varepsilon_0 \gamma}\left(\frac{4}{g_s g_v}\right)^{\frac{1}{2}}$, where γ (=v_f) is the band parameter and ε_0 is the band parameter.

The quasiparticle behaviour of 2D graphene depends crucially on whether the system is doped or not: It has been suggested that the undoped intrinsic graphene is a marginal Fermi liquid and doped graphene with free carriers is invariably a

garden-variety 2D Fermi liquid. The presence of charged impurities in the substrate, unintentional dopants, invariably induce some carriers even in nominally undoped graphene, and the generic behaviour of 2D graphene is likely to be that of a 2D Fermi liquid.

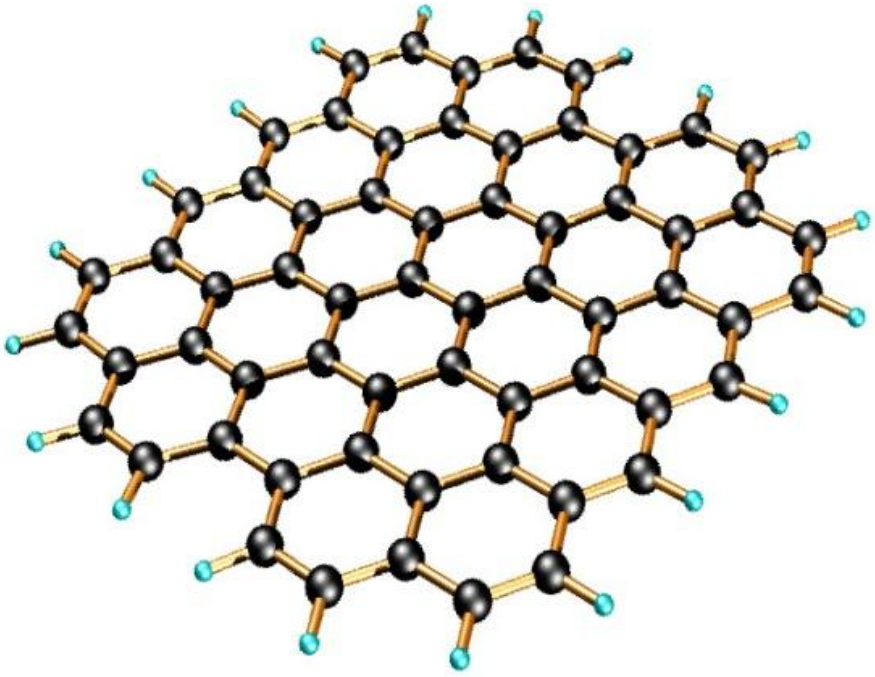

Figure 1.2 2D Graphene sheet composed of hexagonal rings compactly placed next to each other. Black small balls represent carbon atoms.

Figure 1.3 The arrangement of electrons and their relative spin in elemental carbon (left) and in graphene (right) shows the s and two of the p orbitals of the second shell interact covalently to form three sp2 hybrid orbitals. Figure on extreme right displays the sp^2 hybridization model [1].

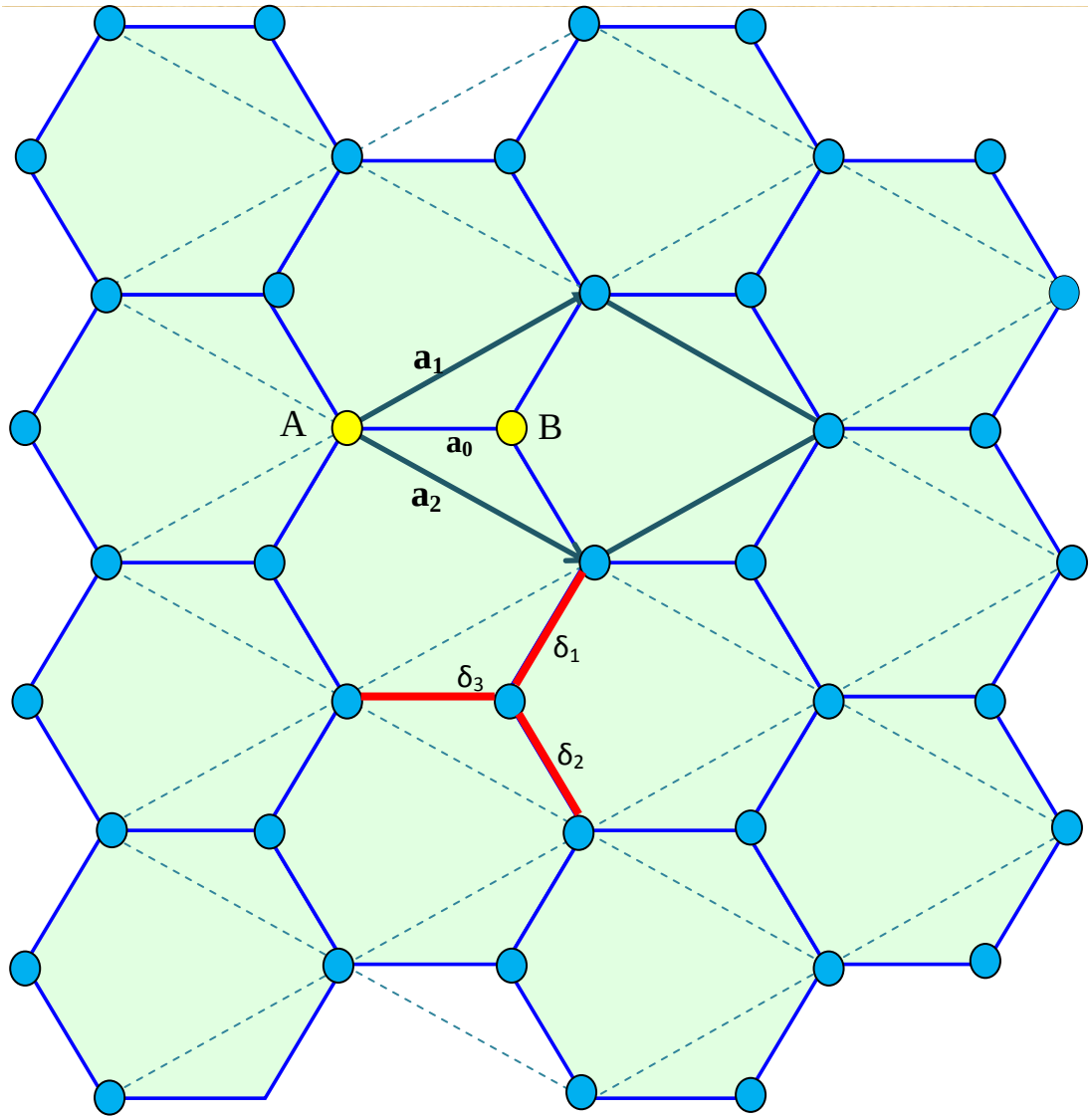

Figure 1.4 A direct lattice of SLG sheet (*green*) with carbon atoms in blue. The Bravias lattice consists of two atoms per unit cell A,B (*Yellow*). This unit cell i.e. the primitive cell is a parallelogram (*dashed blue lines*) with primitive vectors $\mathbf{a_1}$ and $\mathbf{a_2}$ and interstitial distance between two carbon atoms A and B being $a(=a_0) = 1.42$ Å (redrawn with reference to the concept from [1])

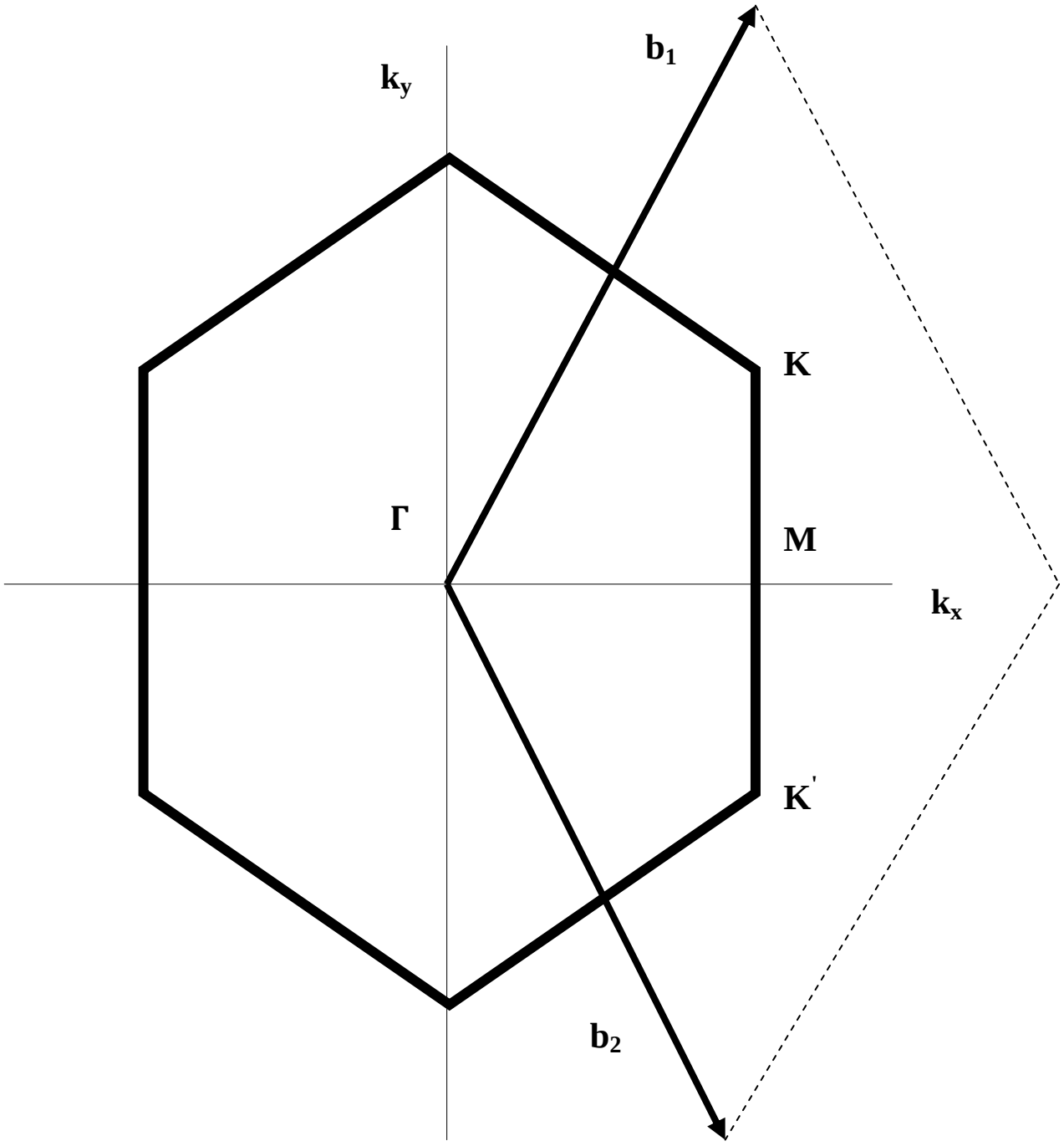

Figure 1.5 Hexagonal Brillioun zone - the reciprocal lattice of Graphene sheet with vectors $\mathbf{b_1}$ and $\mathbf{b_2}$. The Brillouin zone is cornered at **K** points famously known as Dirac points.

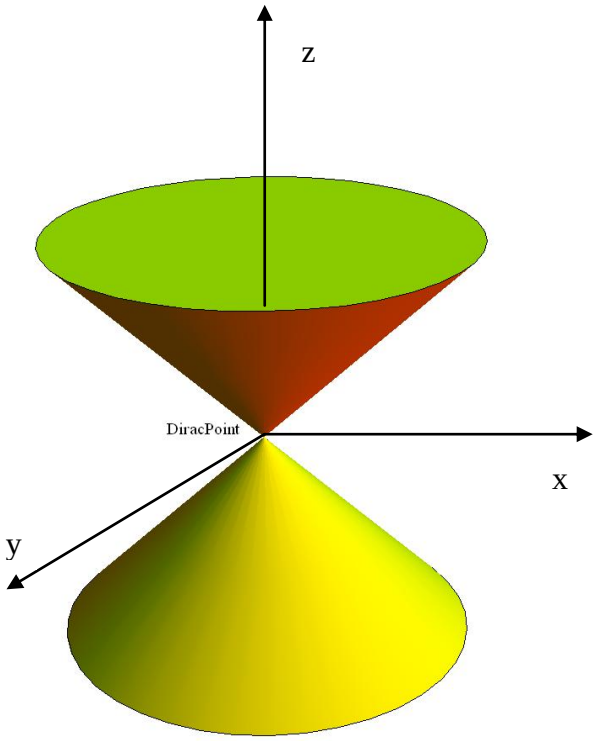

Figure 1.6 Dirac Cone with Dirac point (E_f) at the centre depicting the linear dispersion relation of Graphene and x,y,z representing three axis of the cone.

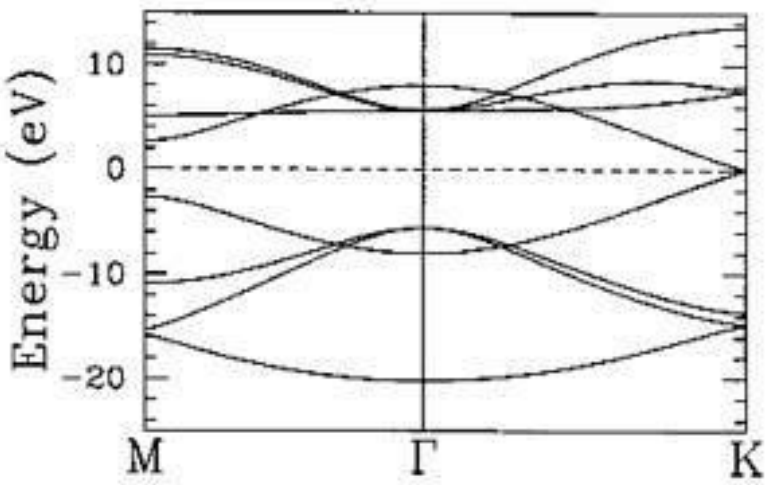

Figure 1.7 Tight Binding band structure of Graphene depicting linear behaviour at **K** points [3]

1.1.2.1 Graphene Evolution and Synthesis

The band structure of graphene was first evaluated in 1946 by Wallace [4], while its linear behavior was observed few years back by S. Y. Zhou et. al. [5] using Angular Resolved Photo emission Spectroscopy (ARPES). Direct observation of relativistic Dirac fermions with linear dispersion near the Brillouin zone (BZ) corner H was seen, which coexist with quasiparticles that have a parabolic dispersion near another Brillouin zone corner **K** were observed. Until its experimental realization in 2004, Graphene have had little importance as application. In 2004 Novoselov and Geim [6] obtained graphene experimentally by mechanical exfoliation technique (repeated peeling) using a simple Scotch Tape leading to groundbreaking development in the field of science and technology. Since then various groups have worked upon to obtain graphene on large scale implementing various experimental methods using top-bottom or bottom-top approach such as Exfoliation and cleavage, Plasma enhanced chemical vapour Deposition techniques, Various chemical methods, Thermal Decomposition of SiC, Thermal Decomposition on other substrates, unzipping CNTs etc. There have been quite good number of review articles on graphene synthesis present in the literature which gives a detailed view on the synthesis of graphene and graphene based systems carried out by several experimentalists, by applying various techniques [7,8]. Graphene due to its unique properties has been used to develop highly efficient materials such as graphene transistors, optoelectronic devices, modulators etc. Majorly, the basic substrate considered for graphene growth/formation is SiO_2 or SiC as per its utility. There have been number of attempts made to grow graphene on SiO_2 substrate.

Novoselov and group [6] synthesized few layer graphene by mechanical exfoliation. They used 1-mm-thick platelets of highly -oriented pyrolytic graphite

(HOPG) with mobility > 100,000cm^2/V.s at 4K. Using dry etching in oxygen plasma, they first prepared 5 mm-deep mesas on top of the platelets (mesas were squares of various sizes from 20 mm to 2 mm). The structured surface was then pressed against a 1-mm-thick layer of a fresh wet photoresist spun over a glass substrate. After baking, the mesas became attached to the photoresist layer, which allowed to cleave them off the rest of the HOPG sample. Then, using scotch tape they started repeatedly peeling flakes of graphite off the mesas. Thin flakes left in the photoresist were released in acetone. When a Si wafer was dipped in the solution and then washed in plenty of water and propanol, some flakes became captured on the wafer's surface (as a substrate, n+-doped Si with a SiO_2 layer on top was used; in order to avoid accidental damage - especially during plasma etching - use a relatively thick SiO_2 was used with t =300nm). This process was followed by ultrasound cleaning in propanol, which removed mostly thick flakes. Thin flakes (d < 10 nm) were found to attach strongly to SiO2, presumably due to van der Waals and/or capillary forces.

Another synthesis with SiO_2 as a substrate was done by Jens Hofrichter and group [9]. They opted for thermally grown SiO_2 on Si with a thickness of 300 nm as the starting material, followed by depositing, 50 nm of amorphous silicon carbide (SiC) onto the silicon dioxide layer by plasma-enhanced chemical vapor deposition (PECVD). After deposition of a 500 nm thick nickel layer by dc magnetron sputtering, the sample is annealed at 1100 °C for 30 s in ambient pressure and nitrogen environment in a rapid thermal annealing (RTA) oven, which results into dissolution of silicon and the carbon of the SiC in the nickel layer. By choosing a nickel layer much thicker than the SiC layer, the silicon from the SiC is only dissolved in nickel or forms substoichiometric silicides. The SiC thin film is

completely consumed by this process. Thus the carbon content in the nickel layer can be controlled by the ratio of SiC to Ni layer thickness. However, experiments lowering the SiC thickness by inverse sputtering indicate that carboneous films are formed but are not of a closed shape thus hindering a wet chemical processing needed for device fabrication and characterization. A certain amount of a solid carbon source has to be present for the formation of a closed layer. The SiO_2 substrate has a chemically and thermally stable interface and does not release any Si atoms into the Ni. When the sample is cooled to room temperature, the carbon segregates to the surface of the Ni layer forming a graphene layer. Successively, the nickel layer with the dissolved silicon was wet chemically removed. The lower chemical stability of substoichiometric silicides allows for the usage of hydrogen fluoride free etchants. In this experiment, the silicon-nickel layer was removed by a nitric acid and hydrogen peroxide containing enchant. Optical microscopy helps in studying the nature of graphene as done by above mentioned groups after the synthesis of graphene.

1.1.3 Bilayer graphene

Bilayer Graphene (BLG) consists of two coupled SLG placed one above other and hence can be considered as building block for 3D stacks of graphene system such as graphite. Its unit cell consists of four atoms. Two atoms, (A_2, B_2) in lower layer and the remaining two atoms (A_1, B_1) in upper layer, arranged in Bernal stacking as shown in fig 1.8 a). Every B_2 site in lower layer lies directly below an A_1 in the upper layer, whereas A_2 and B_1 don't lie directly below or above the site in the other layer [10]. The tight binding model for Bernal bilayers results into Hamiltonian which is a 4x4 matrix with two sublattices, and two layer degrees of freedom and hence the corresponding band structure consists of four nondegenerate bands

(fig 1.8 (b)). It has some fascinating properties, distinct from SLG and 2DEG, even though it resembles some peculiarities of each. The DOS and r_s parameter for BLG differs drastically with that from SLG. These parameters for BLG is mass dependent similar to 2DEG and unlike SLG.

$$D(E) = \frac{g_s g_v m}{2\pi\hbar^2} \tag{1.3}$$

$$r_s = \frac{e^2 m g_s g_v}{2\varepsilon_0 \pi\hbar^2\sqrt{\pi n}} \tag{1.4}$$

These BLG structures can be formed with the same technique used to obtain SLG flakes.

a) **b)**

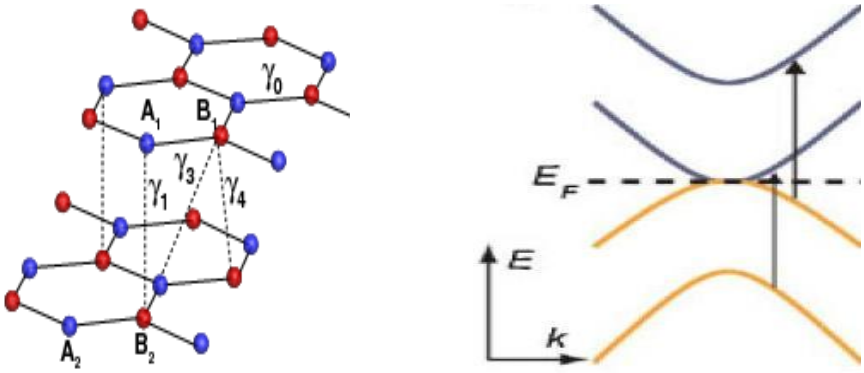

Figure 1.8 Displays **a)** position of carbon atoms in Bilayer graphene **b)** Band Structure of Bilayer Graphene [11]

1.1.4 Gapped Graphene

Graphene because of its unique features has been immensely studied in recent few years. With significant rise in the research based on graphene and its application in industries, the modification in the substance is also being considered by scientists and researchers around the globe. One of it is introducing a gap in between valence and conduction band through various techniques e.g. Spin-Orbit Interaction, Breaking of Sublattice symmetry, External magnetic field, finite geometry effect and various other instabilities. The $E \to \vec{k}$ relation of gapped graphene differs from that of SLG by a value of Δ [12,13]

i.e.

$$E(\vec{k}) = \sqrt{\hbar^2 v_f^2 k^2 + \Delta^2} \tag{1.5}$$

The band structure of gapped graphene differs from SLG drastically. While the band structure of SLG is linear in nature the band structure of Gapped Graphene is Parabolic as can be seen from fig. 1.9. Devices based on gapped graphene have better working efficiency compared to semiconductor devices because of presence of gap as it provides way to have on-off ratio in contrast to graphene, and thus can be considered as a better substitute to 2DEG semiconductors. The density of states, at Fermi Energy, for gapped graphene differs by the factor $\sqrt{1 + \frac{\Delta^2}{E_f^2}}$ from that of SLG.

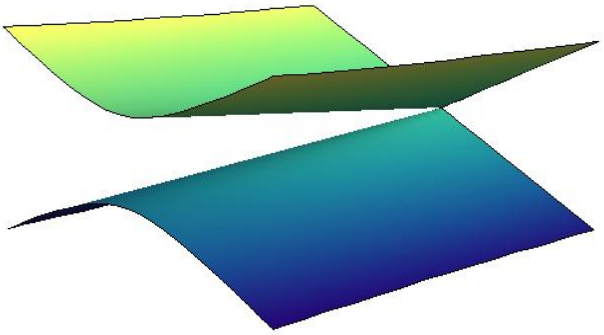

Figure 1.9 3D Band structure of Gapped graphene. Moving from front to back the value of Δ (gap) decreases, changing the shape of band structure from parabola to linear.

Table 1: Comparison of various quantities and parameters of 2DEG, graphene and graphene based systems

	SLG	*Gapped Graphene*	*BLG*	*2DEG*
Energy Spectrum $(E_{\vec{k}})$	$\hbar v_f \lvert\overrightarrow{k}\rvert$	$\sqrt{\vec{k}^2 + \Delta^2}$	$\frac{\hbar^2\vec{k}^2}{2m}$	$\frac{\hbar^2\vec{k}^2}{2m}$
Fermi energy E_f	$\hbar v_f\sqrt{n\pi}$	$\sqrt{\mu^2 - \Delta^2}$	$\frac{2\pi\hbar^2 n}{m g_s g_v}$	$\frac{2\pi\hbar^2 n}{m g_s g_v}$
D(E) Density of States	$\frac{g_s g_v E}{2\pi(\hbar v_f)^2}$	$\frac{g_s g_v E}{2\pi(\hbar v_f)^2}$	$\frac{g_s g_v m}{2\pi\hbar^2}$	$\frac{g_s g_v m}{2\pi\hbar^2}$
$D_0 = D(E_f)$ *Density of states at Fermi Energy*	$\frac{\sqrt{g_s g_v n}}{\sqrt{\pi}\hbar v_f}$	$\frac{\sqrt{g_s g_v n}}{\sqrt{\pi}\hbar v_f}\sqrt{1 + \frac{\Delta^2}{E_f^2}}$	$\frac{g_s g_v m}{2\pi\hbar^2}$	$\frac{g_s g_v m}{2\pi\hbar^2}$
r_s *Interaction Parameter*	$\frac{e^2}{\varepsilon\hbar v_f}\frac{\sqrt{g_s g_v}}{2}$	$\frac{e^2}{\varepsilon\hbar v_f}\frac{\sqrt{g_s g_v}}{2}$	$\frac{2me^2}{\varepsilon\hbar^2\sqrt{n\pi}}$	$\frac{me^2 g_s g_v}{2\varepsilon\hbar^2\sqrt{n\pi}}$
q_{TF} *Thomas-Fermi wave-vector*	$\frac{\sqrt{4\pi g_s g_v n}e^2}{\varepsilon\hbar v_f}$	$\frac{\sqrt{4\pi g_s g_v n}e^2}{\varepsilon\hbar v_f}$	$\frac{me^2 g_s g_v}{\varepsilon\hbar^2}$	$\frac{me^2 g_s g_v}{\varepsilon\hbar^2}$
q_s	$\frac{e^2 g_s g_v}{\varepsilon\hbar v_f}$	$\frac{e^2 g_s g_v}{\varepsilon\hbar v_f}$	$\frac{me^2(g_s g_v)^{\frac{3}{2}}}{\varepsilon\hbar^2\sqrt{4\pi n}}$	$\frac{me^2(g_s g_v)^{\frac{3}{2}}}{\varepsilon\hbar^2\sqrt{4\pi n}}$
$F_{ss'}$	$\frac{1}{2}\{1 + \cos\theta_{kk'}\}$	$\frac{1}{2}\{1 + \cos\theta_{kk'}\}$	$\frac{1}{2}\{1 + ss'\cos(2\theta_{k,k+q}\}$	1
$\omega_p(q)$ *Plasmon dispersion*	$\left(\frac{e^2 v_f q}{\varepsilon\hbar}\sqrt{\pi n g_s g_v}\right)^{\frac{1}{2}}$	$\left(\frac{e^2 v_f q}{\varepsilon\hbar}\sqrt{\pi n g_s g_v}\right)^{\frac{1}{2}}$	$\sqrt{\frac{2\pi ne^2}{\varepsilon m}q}$	$\sqrt{\frac{2\pi ne^2}{\varepsilon m}q}$

1.1.5 Graphene Superlattice

An interest has been sparked off in graphene based multilayer (GBM) and Graphene superlattice (GBS) structures because of their potential applications in technology and there have been extensive investigations, experimental as well as

theoretical, on GBS and GBM in recent past. Unique properties of graphene, inspired to think that graphene based multilayer and superlattice structures stand a better chance of application in various industries. The interlayer interactions are strong enough to make it a better component that can be utilized in developing efficient electronic devices. A superlattice structure is the stack of layers of two (or more) different materials arranged periodically one above another. The thickness between two consecutive layers ranges from micro to nanometers. These superlattice layers may have similar or different charge density and mass. This type of modified structures can be of great scientific and technological application, because of the enhancement in properties and work efficiency as compared to original crystal structures. Superlattice structures can be experimentally realized with the help of molecular beam epitaxy (MBE), sputtering techniques etc. The study of GBS helps to analyze the experimental study of Raman spectroscopy which characterizes the superlattice systems [14]. Change in the properties can be attributed to the change in band structure of the superlattice. This Superlattice structure can be viewed as a quantum well structure Fig 1.10.

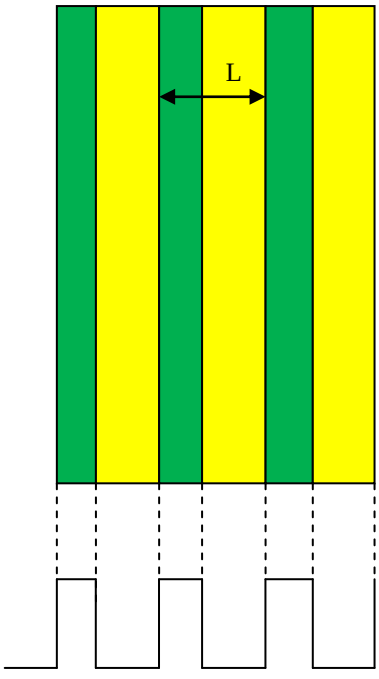

Figure 1.10 Alternate layers of graphene (green) and SiO_2 (yellow) with a period of width L, resembling the quantum well (below) structure

The development in the field of nanoscience is fuelled by observed unusual properties of nanometer size matter, which may be exploited to improve the performance in various applications such as optics, microelectronics, thermo electrics and magnetics. There has been tremendous interest in understanding properties of Graphene because of its technological applications. Ever since its experimental realization, graphene has aroused a great deal of interest because of the novel physics which it exhibits and also because of its promising potential as a new material for technological innovations and applications. Its high electrical conductivity and high optical transparency make it a potential candidate for transparent conducting electrodes required for applications such as touchscreens, liquid crystal displays, organic photovoltaic cells and organic light-emitting diodes, solar cells. There is a need to provide theoretical interpretation and feedback to experimental measurements, to predict device characteristics, and to provide a basis for the functional progress of new devices. All these devices need to have a better understanding of physical properties and quantities before they can be well modified and engineered so as to have better operating devices.

1.2 Many Particle Aspects

To study the low dimensional system (dimension less than or equal to 2) in detail it is appropriate to model it in terms of electron gas/liquid picture.The Many-body theory provides the framework for understanding the collective behavior of vast assemblies of interacting particles and the changes induced by these effects on a given system. These effects are relevant only in systems containing large numbers of constituents and its study can be extremely complex because the motions of particles are intricate. Many particle theory paves way to understand various properties such

as collective excitations, exchange and correlation, scattering, screening, energy levels, susceptibility, superconductivity, ground state properties etc.

Graphene has spawned tremendous interest and activity in studying the properties of this unique system of 2DEG. Because of the different energy band dispersions, screening properties in graphene exhibit significantly different behavior from the conventional 2D systems. Though, there have been some calculations on dynamical screening and collective excitations in graphene which consists of fermions following Dirac equation. Recent experiments on transport in graphene layers have validated extensive theoretical efforts directed at understanding various properties of two-dimensional Dirac fermions. Interaction among many particles gives rise to some fascinating qualities/properties of a system like screening, collective excitations, band structure, structure factor, pair correlation function, self energy, exchange interaction, compressibility, energy loss etc. Several papers have been published on the transport and spectroscopic measurements, which has led to rapidly flourish experimental and theoretical interest in this field. Aaron Bostwick, Taisuke Ohta, Thomas Seyller, Karsten Horn and Eli Rotenberg [15] pointed that the linear spectrum manifests subtle many-body renormalization effects, preserving, however, the Landau Fermi liquid quasiparticle picture by performing ARPES experiment. Their findings reflect that electron–plasmon coupling plays an unusually strong role in renormalizing the bands around the Dirac crossing energy—analogous to mass renormalization by electron–boson coupling in ordinary metals and that electron–electron, electron–plasmon and electron–phonon coupling must be considered on an equal footing in attempts to understand the dynamics of quasiparticles in graphene and related systems. Infrared spectromicroscopy study was conducted of charge dynamics in graphene integrated in gated devices. Several

observations reported in this paper indicate the relevance of many-body interactions to the electromagnetic response of graphene [16]**.** Ab-initio simulations of the ARPES spectra of graphene were performed including electron-electron and electron-phonon interactions where the results were compatible with experimental results on many-body effects. ARPES is a powerful experimental technique for directly probing electron dynamics in solids. The energy versus momentum dispersion relations and the associated spectral broadenings measured by ARPES provide a wealth of information on quantum many-body interaction effects. In particular, ARPES allows studies of the Coulomb interaction among electrons (electron-electron interactions) and the interaction between electrons and lattice vibrations (electron-phonon interactions) [17]. On the theoretical side, there has been a number of works in the literature on the effects of electron-electron interaction in graphene. The influence of electron-electron scattering on quasiparticle lifetimes in graphite was calculated by J. González, F. Guinea, and M. A. H. Vozmediano [18]. Many body interaction effects in undoped and doped graphene were studied by Das Sarma and group. There studies reveal that extrinsic graphene shows no deviation from Fermi-Liquid behaviour while undoped graphene shows a marginal Fermi Liquid behaviour at the Dirac point, concluding real Graphene to be a Fermi liquid [19]. Theoretical calculations for the quasiparticle lifetime, renormalization factor, and effective velocity for both the doped and the undoped cases have been performed. It has been suggested that extrinsic graphene manifests a Fermi liquid behavior similar to the regular 2D electron gas, indicating that the quasiparticle description is indeed valid, While E.H. Hwang, Ben Yu-Kuang Hu, S. Das Sarma calculated electron-electron induced quasiparticle self-energy and spectral function in graphene layer within dynamical-screening approximation. The

spectral function indicates extrinsic graphene to be a Fermi liquid. They have also calculated hot carrier inelastic scattering due to electron-electron interaction highlighting the fact that the linear dispersion and chiral property of graphene give lifetime energy dependences that are qualitatively different from those of parabolic-band semiconductors [20]. Influence of electron-electron interaction on the one-particle Green's function of a doped graphene sheet based on the RPA and on graphene's massless Dirac equation continuum model was studied by Marco Polini, Reza Asgari, Giovanni Borghi, Yafis Barlas, T. Pereg-Barnea, and A. H. MacDonald [21]. The results indicate that states near the Dirac point interact strongly with plasmons with a characteristic frequency that scales with the sheet's Fermi energy and depends on its interaction coupling constant, partially explaining prominent features of recent angle-resolved photoemission spectroscopy data. Effect of electron-electron interaction on Fermi energy, including short-range and long-range interactions was studied by R.Roldan and group [22]. Van der Walls effect (Casimir interactions) were studied for graphene based systems by B. E. Sernelius [23] and Jalal Sarabadani, Ali Naji, Reza Asgari, and Rudolf Podgornik [24] These effects are the results of many-body interactions. Moreover there has been a study in past revealing how many-body effects control the orbital magnetic susceptibility (OMS) making doped graphene a unique system to explore [25]. Their theory shows that doped graphene sheets have a very intriguing orbital magnetic response. If electron-electron interactions are neglected, the OMS is identically zero. When electron-electron interactions are taken into account, the OMS turns out to be finite controlling the orbital response. Weakly interacting doped graphene sheets are thus many-body orbital paramagnets.

The electron self-energy as well as the quasiparticle spectral function in doped graphene was calculated, taking into account electron-electron interaction in the leading order dynamically screened Coulomb coupling and electron-impurity interaction associated with quenched disorder. The theory provides the basis for calculating all one-electron properties of extrinsic graphene. Comparison with existing ARPES measurements shows broad qualitative and semiquantitative agreement between theory and experiment, for both the momentum-distribution and energy-distribution curves in the measured spectra [26]. A brief summary of electron-electron interaction in graphene was made by Bruno Uchao [27] and group emphasizing the importance of electron-electron renormalization effects in experiments as well as the fine structure constant. Moreover there have been excellent review articles based on many body interactions in grpahene and graphene based systems, discussing the characteristics arising due to electron-electron interactions [28-31]. The interactions amongst the particles are present in almost all areas of physics and leads to plethora of effects ranging from ground state properties to excited states. Many particle aspects play an important role in understanding essential properties of low dimensional systems. Properties involving many particle interactions for graphene qualitatively differ from those for normal 2DEG, observed in systems like semiconductor hetero structures and MOSFETs. The electrons in a system interact via long-range Coulomb interactions. The electron-electron interaction strongly modifies the free electron picture which is commonly used to describe various systems. There has been number of works in the literature on the effects of electron-electron interaction in graphene. However explicit results for doped graphene were still lacking, which would help us to interpret various important physical quantities like scattering, excitation spectrum, paramagnetism,

ferromagnetism, carrier mobility, thermal conductivity, fermi liquid state etc of the graphene systems. This motivated us to investigate the many particle aspects of graphene using standard mathematical formalism.

1.3 Essential theoretical Formalism

1.3.1 Density-density response function

When a system with certain density is perturbed with onset of some external density, it leads to density fluctuation due to disturbances created. It is important to conceptualize this response of the system to understand basic character of material. A physical quantity of crucial utility in the understanding of the many body properties of condensed matter is the dynamic electron density-density response function χ. Many body properties like ground state energy, electron-electron and transport scattering rate, collective excitations, compressibility, structure factor, pair correlation function etc are all calculated using this response function. A general concept of this response function is already available in literature. For a review it is stated briefly as below:

The density response of the system to an external potential is given as

$$\int(-e)V_{ext}(\vec{\mathrm{r}},t)\hat{n}(\vec{\mathrm{r}})d\vec{\mathrm{r}} = \int(-e)V_{ext}(\vec{\mathrm{q}},t)\hat{n}^{+}(\vec{\mathrm{q}})d\vec{\mathrm{q}} \tag{1.6}$$

Where $\hat{n}(\vec{\mathrm{r}})$ is the number operator for particles at $\vec{r}$

$$\hat{n}(\vec{\mathrm{r}}) = \sum_{i} \delta(\vec{\mathrm{r}} - \vec{\mathrm{r}_i}) \tag{1.7}$$

i denotes position vector of ith electron.

The induced charge density $n_1(r,t)$ and external potential $V_{ext}(r,t)$ is given as [32]

$$n_1(\vec{\mathrm{R}},t)=\int_0^{\infty}d\tau\int d\vec{\mathrm{R}'}\chi_{nn}(\vec{\mathrm{R}},\vec{\mathrm{R}'},\tau)V_{ext}(\vec{\mathrm{R}'},t-\tau) \tag{1.8}$$

$$V_{ext}(\vec{\mathrm{r}'},t)=\frac{1}{L^d}V_{ext}(\vec{\mathrm{q}'},\omega)\,e^{i(\vec{\mathrm{q}'}\cdot\vec{\mathrm{r}'}-\omega t)} \tag{1.9}$$

Combining eq. (1.8) and (1.9) we have

$$n_1(\vec{\mathrm{r}},t)=\frac{1}{L^d}\sum_{\boldsymbol{q}}n_1(\vec{\mathrm{q}},\omega)e^{i(\vec{\mathrm{q}}\cdot\vec{\mathrm{r}}-\omega t)} \tag{1.10}$$

Where

$$n_1(\vec{\mathrm{q}},\omega)=\chi_{nn}(\vec{\mathrm{q}},\vec{\mathrm{q}}',\omega)V_{ext}(\vec{\mathrm{q}}',\omega) \tag{1.11}$$

In general the relation between induced charge density and external potential can be written as

$$n_1(\vec{\mathrm{Q}},\omega)=\chi_{nn}(\vec{\mathrm{Q}},\omega)V_{ext}(\vec{\mathrm{Q}},\omega) \tag{1.12}$$

where $\chi_{nn}(\vec{\mathrm{q}},\omega)$ is the density-density response function. The perturbation caused by external potential is linearly proportional to induced charged density. Here it is assumed that the perturbation is small so that the reponse of the system is linear function of the perturbation. The main objective of linear response theory (LRT) is to obtain this function. Experimentally, the interaction of probe with the electrons is regarded as a small perturbation. Thus the results of these experiments can be considered as properties of unperturbed system [32].

1.3.2 RPA bare bubble diagram

Using Feynman diagrammatic techniques one can directly calculate the density-density response function χ_{nn}

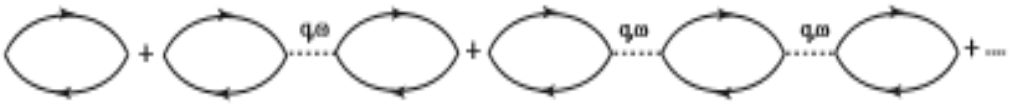

Figure 1.11 Infinite series of Feynman diagrams corresponding to the RPA for $\chi_{nn}(q,\omega)$ [32]

$$\chi^{RPA}(\vec{q},\omega) = \chi_0(\vec{q},\omega) + V_{\vec{q}}[\chi_0(\vec{q},\omega)]^2 + V_{\vec{q}}{}^2[\chi_0(\vec{q},\omega)]^3 + \cdots$$

$$= \frac{\chi_0(\vec{q},\omega)}{1-V_{\vec{q}}\chi_0(\vec{q},\omega)} \tag{1.13}$$

Where the denominator of eq. 1.13 is the dynamic dielectric function given as

$$\epsilon(\vec{q},\omega) = 1 - V_{\vec{q}}\,\chi_0(\vec{q},\omega) \tag{1.14}$$

Where $\chi_0(q,\omega)$ is the dynamic polarizability given as [2]

$$\chi_0(\vec{q},\omega) = -\frac{g_s g_v}{L^2}\sum_{\mathbf{k}ss'}\frac{f_{s\mathbf{k}} - f_{s'\mathbf{k}'}}{\omega + \epsilon_{s\mathbf{k}} - \epsilon_{s'\mathbf{k}'} + i\eta}F_{ss'}(\vec{\mathrm{k}},\vec{\mathrm{k}'}) \tag{1.15}$$

Where $\vec{\mathrm{k}'} = \vec{\mathrm{k}} + \vec{\mathrm{q}}$, $s, s' = \pm 1$ denote the band indices and $F_{ss'}(\vec{\mathrm{k}},\vec{\mathrm{k}'})$ is the overlap of the states which follows different expression for SLG,BLG, Gapped graphene and 2DEG. The $\chi_0(\vec{q},\omega)$ for 2DEG, SLG and BLG differs drastically. This change in the polarization function changes the response of the system to external perturbation.

One of the most successful and widely accepted approaches to solve the problem of screening has been the random-phase approximation (RPA). The RPA is a many body theoretic method by which quantitative predictions beyond the Hartree–Fock model can be made. In this approximation it is assumed that only

single-particle excitations of the same wave vector as the Coulomb interaction plays an effective role in the screening process while the effects of others having different wave vectors cancel out. Use of the RPA is justified when the electron-electron interaction is strong enough that quantum coherence does not dominate. In the past years, there have been several studies on Coulomb screening and the collective excitation spectrum in the monolayer graphene using the RPA. It appears from the existing literature that no calculation has been performed beyond RPA.

1.4 Dielectric function

The dielectric function (Eq. 1.14) gives physics of the system making it easy to gain knowledge about the ground state properties and the spectrum of collective excitations and explains electron-energy-loss experiments. The dielectric function helps in obtaining major properties of the system directly, such as collective excitations, energy loss, stopping power, dynamic structure factor, pair correlation function, wake effects, self energy, screening charge density etc. Several authors have reported the usefulness of this function in past. It is usually defined for arbitrary wave function, frequency, temperature, doping. E.H.Hwang and S. Das Sarma [2] calculated the dynamical dielectric function $\epsilon(\vec{q},\omega)$ of SLG at arbitrary wave vector q and frequency ω, in the self-consistent-field approximation, at zero temperature. The results were then used to find the dispersion of the plasmon mode and the electrostatic screening of the Coulomb interaction in 2D graphene layer while similar work was reported by [33] obtaining the screening charge density, dispersion relation and decay rate of plasmons and acoustic phonons as a function of doping. Dynamic dielectric function for bilayer graphene and gapped graphene was calculated within RPA [12, 13, 34]. Moreover the density-response function of

Bilayer graphene using the four band linear response model was evaluated by G. Borghi, Marco Polini, Reza Asgari, and A. H. MacDonald [35] while the static polarization function using two band model within RPA was evaluated to discuss dielectric properties, screening, the Kohn anomaly, Freidel oscillations and RKKY interactions by Hwang *et.al.* [36]. Jia-Ning Zhang evaluated static polarization function for gapped graphene to analyze the screening effect and density at finite temperature and density [37]. The screened potential due to charged impurities was obtained in static limit of dielectric function by [38]. The electromagnetic response of graphene, expressed by the dielectric function, and the spectrum of collective excitations were studied as a function of wave vector and frequency by A.Hill et al [39]. Reflectance and transmission as well as dynamical conductivity for a system can also be studied using the dielectric function [40].

The static polarization function has been obtained by Tsuneya Ando to obtain the conductivity of graphene at various temperatures [41]. The vacuum polarization charge distribution was studied by Valeri N. Kotov, Vitor M. Pereira, and Bruno Uchoa [30] while, Chirality and Correlations were obtained by Yafis Barlas, T. Pereg-Barnea, Marco Polini, Reza Asgari, and A. H. MacDonald [42] using dynamic dielectric function**.** Moreover *f*-sum rule and unconventional spectral weight transfer in graphene were obtained by J. Sabio, J. Nilsson, and A. H. Castro Neto implementing density-density response function. The *f*-sum rule provides strong constraints for theories of interacting electrons in graphene [43]. Temperature dependent polarization function was used to obtain the transport properties in graphene [44]. Density-Density response function has been evaluated to obtain palsmon dispersion, Drude weigth and a.c. conductivity in doped graphene sheets by Saeed.H. Abedinpour et.al. [45,46].

1.4.1 Work done in past

1.4.1.1 Structure factor and pair correlation function

The Dynamic structure factor also known as form factor provides useful and maximum information about the scattering as well as the density excitation spectrum of a system. Theoretical Evaluation of structure factor for a system can act as a useful tool for the experimentalists to analyse their results.

Mathematically the Dynamic $S(\vec{q},\omega)$ and static $S(\vec{q})$ structure factor can be written as [47]

$$S(\vec{q},\omega) = \frac{1}{n\pi}\frac{\epsilon_2(\vec{q},\omega)}{\epsilon_1^2(\vec{q},\omega)+\epsilon_2^2(\vec{q},\omega)} \tag{1.16}$$

$$S(\vec{q}) = \int S(\vec{q},\omega)\, d\omega \tag{1.17}$$

where $\epsilon_1(\vec{q},\omega)$ and $\epsilon_2(\vec{q},\omega)$ are the imaginary and real parts of dynamic dielectric function defined in eq. 1.14.

The Dynamic structure factor of 2DEG has been calculated by using various approximation methods. Tanatar *et.al.* [48] has evaluated density-density response function and dielectric function i.e. $\chi(\vec{q},\omega)$ and $\epsilon(\vec{q},\omega)$ using memory-function formalism. The Dynamic structure factor displays a broad-peak structure at a particular value of wave-vector q at different values of r_s and hence no evidence of plasmons was found for the q values investigated. This theory of finding a single-broad-peak structure was later defied by Moudgil and group [49] with appearance of 2 broad peaks within intermediate q values, whereas Darren J.T. Leonard and Neil F. Johnson [50] has obtained dynamical structure factor in a magnetic field using Chern-Simons theory of composite fermions. It is shown that dynamic structure

factor has major influence on the spectral function of the probe. They have also proposed an experimental method to determine the composite fermion effective mass via a tunneling experiment which directly measures the spectral function. B Tanatar and D.M. Ceperley [51] has used Variational and fixed-node Green's-function Monte Carlo calculations to obtain the ground state properties of 2DEG like pair distribution function and static structure factor for different values of interaction parameter.

First-order Feynman diagrams for the proper polarizability of a two-dimensional electron liquid in the jellium model, valid for arbitrary wave vector and frequency, are evaluated, their singularities and analytical properties are examined, and a reliable numerical procedure for calculating them is established. Quantities such as the $\varepsilon(\vec{q},\omega)$, $S(\vec{q},\omega)$, $S(\vec{q})$, and the pair correlation function $g(\vec{r})$ have been calculated and compared with the corresponding quantities in the RPA. Comparison has also been made with the three-dimensional case. A closed expression for the plasmon dispersion within the RPA has been derived. The first-order theory interestingly enough predicts a large enhancement of the static polarizability for $q=2k_f$, which could play an important role in predicting charge-density-wave instabilities in metallic layered compounds [52]. The density-density response of the 2DEG is obtained at zero temperature by solving the Dyson equation for the particle-hole Green's function, including exchange Coulomb matrix elements and short-range contributions in the ladder approximation. The effect of these correlations on the static structure factor and pair-correlation function has been studied and the results are compared with the normal random-phase approximation, local field theories and quantum Monte Carlo calculations [53]. Moreover, G Barnea [54] has derived general theory of dynamic structure factor of an electron gas. His theory is a close

support to the inelastic x-ray scattering experiments where the spectrum can be clearly seen to have two sharp peaks, providing the evidence of existence of plasmons at intermediate values of *q*, in two dimensional systems. All the above mentioned theory and observations in case of 2DEG are important to speculate minor features of the conventional 2D graphene too, as it has its some own unique properties which can provide a way to develop new materials with better efficiency. This motivated us to perform the calculations to find out dynamic and static structure factor and pair correlation function of graphene as no work has been reported in literature earlier on the topics using density-density response function. The static structure factor of graphene in presence of magnetic field has been obtained by K. Shiyuza [55]. The author has reported that for graphene even the vacuum state has a nonzero density spectral weight, which, together with the structure factor for all frequencies, grows significantly with increasing wave vector; such unusual features of density correlations are a ”relativistic” effect deriving from massless Dirac quasiparticles in graphene. The pair correlation function for a system is defined as probability of finding a particle if one is present already at origin. It is directly related to static structure factor [47]. The pair correlation function has been evaluated by Dharma Wardana [57] using first-principle calculations through which exchange-energy has been obtained. For graphene based systems there have been several attempts made to investigate the ground state properties. D. S. L. Abergel and Tapash Chakraborty [58] evaluated pair correlation function as well as corresponding structure factor for Bilayer graphene concluding that it resembles the quantities obtained for 2DEG and that the results hold true for all Dirac based systems with filled valence band.

1.4.1.2 *Screening charge density and screened potential*

When a positive charge is placed in an electron gas, the electrons gather around the charge tries to compensate for the electrostatic potential it has induced. The phenomenon is known as screening and it is one of the simplest and most important manifestations of electron-electron interaction [59]. The system tries to nullify this perturbation effect by gathering around the particle and will continue to gather till its effect is completely neutralized. The amount of charge to neutralize the effect is termed as screening charge density. The problem of screening of an external charge is important in view of transport properties of graphene keeping in mind its technological applications. Various theoretical models have been developed on the basis of above concept. The screening in graphene based systems has been studied by authors by considering the external charge as Coulomb impurity either away from the plane or inside the plane.

Freidel Oscillations have been an important observation while investigating screening, screening charge density and screened potential for 2DEG and Graphene based systems. These Oscillations can be a useful tool to detect microscopic disorder. Mathematically these oscillations occur due to discontinuity in the derivative and can be considered as signature of Fermi-liquid state [60-62]. Ivan S. Terekhov [63] and group has studied screening in supercritical and subcritical regime taking into account electron-electron interactions in Hartree Approximation.

1.4.1.3 *Self Energy*

A bare particle in a system interacts with itself via many-body system thereby disturbing its own energy which is termed as self-energy. The particle interacts with

other particles creating a cloud and this cloud in turn creates impact on the particle disturbing its motion [64]. Single-particle spectral function, associated mean free paths, quasiparticle properties, such as inelastic quasiparticle lifetimes quasiparticle decay, renormalization factor, and renormalization velocity can be studied by knowing electron self-energy. Self-energy can also be used to obtain ARPES spectra which have been reported by a host of authors for graphene.

Self-Energy has been evaluated for 2DEG by using various tools. J.J. Quinn and Richard A. Ferrell obtained self-energyby making use of Lindhard's frequency and wave-number dependent dielectric constant [65] while self-energy of a positron in an electron Fermi sea was calculated by G C Aers and J B Pendry within the Random Phase approximation [66]. Self energy for layered 2DEG was evaluated by Yu. M. Malozovsky and S.M. Bose and P.Longe using Fermi Liquid approach [67].

Many body interaction effects was considered to debate on the Fermi liquid vs. the Non-Fermi liquid behavior of SLG by calculating the Self-Energy of the system. S. Das Sarma, E. H. Hwang, and Wang-Kong Tse [19]. Self –energy as well as the quasiparticle spectral function in doped graphene was evaluated by taking into account electron-electron interaction in the leading order dynamically screened Coulomb coupling and electron-impurity interaction [26]. Carrying forward their theory many one-electron properties of extrinsic graphene can be calculated. Lifetime and associated mean free paths were evaluated using dynamically screened Coulomg interaction within RPA at zero-temperature [68]. Self-energy and single particle spectral function of Bilayer graphene was obtained using GW approximation in the low energy limit with the two band model [69].

1.4.1.4 *Compressibility*

Compressibility $\kappa^{-1} = \frac{\partial \mu}{\partial n}$ is a fundamental physical quantity that is intimately related to the strength of inter-electron interactions. Compressibility is an important phenomenon to understand the ground state of any system as it provides important information about electron correlation, chemical potential, stability of the system etc. [31]. There has been literature published on electronic compressibility of graphene for monlayer and bilayer graphene. The results in case of monolayer graphene indicate exchange and correlation effects completely cancel out each other or are negligible. Experimentally it was proved by [70] which was in contrast to the theoretical model given by D.E. Sheehy and J. Schmalian [71]. But the theory developed by Abergel et.al. approved the experimental results proving the exchange correlation cancellation, while in bilayer graphene the cancellation of energies donot take place [72]. There have been number of papers published on compressibility of monolayer and bilayer graphene for zero temperature as well as non-zero temperature [73-75].

1.4.1.5 *Energy loss*

Energy loss suffered by the moving charged particle above a system has gained importance in past years. This physical phenomenon is of great utility to characterize the probing instrument as well as the given system. Basic contribution comes from particle-hole and plasmons. The energy loss is determined by imaginary part of dynamic dielectric function [76].

$$\delta E = Im(\frac{-1}{\epsilon(\vec{q},\omega)}) \tag{1.18}$$

The Electron energy loss (EEL) has been studied for parallel and perpendicular cases of moving particles, by host of authors. Study of collective excitations such as plasma has been reviewed by N.J.M Horing. Electron loss spectroscopy for SLG subject to both parallel and perpendicular particle probe of its dynamical non-local response properties are also treated. [77]. Vassilios fessatidis et.al.[78] has studied the power loss and stopping power for motion of charged particle parallel to the SLG as a function of distance from the graphene plane and of its velocity including the effects of particle-hole and plasmon. The energy loss of charged particle moving parallel to gapped graphene sheet and that of double layer graphene has been studied numerically by Godfrey Gumbs and group [79]. They have observed characteristics difference between response dynamics of SLG and gapped graphene system, though this paper still lacked an analytical support to their numerical results. I. Radovic, L.J. Hadzievski and Z L Miskovic [80] computed stopping and image forces on slow ions moving parallel to supported graphene under gating conditions. The effects of temperature and gate potential are included by means of single scaling parameter as well as the gap in between the graphene layer and substrate has also been considered explicitly in modelling of polarization of graphene which is described by means of Vlasov equations in the relaxation-time approximation. Response of 2DEG has been obtained by A.Bergara, J.M. Pitarke and P. M. Echenique considering example of stopping power for a 2DEG for charge particle moving at a fixed distance from 2D plasma [81]. Energy-loss rates of heavy and light charged particles in a 2DEG at zero temperature are calculated by A.Bergara, I.Nagy and P.M.Echenique. The transition probability per unit time, contributions from electron-hole and collective excitations to the energy loss is obtained within RPA using linear response function. A Kinematical effect that

influences the high-velocity form of the loss rate for different masses of the projectiles is pointed out [82]. Energy loss of energetic ions moving near a solid surface was evaluated by R Nunez, P.M. Echenique and R.H.Ritchie. Emphasis was made on the case of an ion moving with velocity less than that of electrons in the solid. At large distances from the surface it is seen that the contribution of collective excitation always dominated that from particle-hole excitations [83].

1.4.1.6 *Wake effects*

Wake effect is the disturbance caused in a medium by moving external particle or an object in motion, outside the medium. The charge induced by this external charge can be calculated using an appropriate methodology. The visible example of wake effect is wake oscillations created by a travelling boat in a sea with the waves trailing beind the boat. There has been numbers of papers published in literature on wake effects for 2DEG systems. Wake effects arising because of a charged particle moving above the system have been considered in two dimensional quantum electron gases (2DQEG). These effects have been studied using linearized quantum hydrodynamic theory (QHD) by Chun-Zhi Li, Yuan-Hong Song, You-Nian Wang [84]. The quantum statistical and quantum diffraction effects have been included and the induced potential and perturbed density has been evaluated as a function of projectile velocity, particle position and density function. The effects of substrate phonons on image force, stopping potential and wake effects has been reported by I. Radovic,V Borka Jovanovic, D. Borka, Z. L. Miskovic for slowly moving charges above SLG. [85]. Their studies report that oscillations due to wake effects and wake potential gets strongly influenced by the substrate phonons due to coupling with plasmons in graphene and that these studies will help in experimental

study of HREELS or ion trajectories in surface grazing scattering investigations.

The dielectric-response formalism has been used to evaluate the induced density of charge carriers in supported graphene due to an external moving charged particle in terms of its velocity and distance from graphene for several equilibrium charge carrier densities due to graphene doping [86]. It has been found out that, when the particle speed exceeds a threshold value, an oscillatory wake effect develops in the induced charge density trailing the particle. Moreover strong effects are observed in the wake pattern due to finite size of the graphene–substrate gap, as well as due to strong coupling effects, and plasmon damping of graphene's π electrons. You-Nain Wang and Teng-Caj Ma [87] has investigated the wake potential, the induced electron density, and the stopping power for a charged particle moving through a strongly coupled two-dimensional electron gas using linear-response dielectric theory. The influence of the exchange-correlation interaction of electrons has been studied by using a local-field-corrected dielectric function. It has been observed that in the wake potential, the induced electron gas density enhances with the electron-correlation interaction for larger values of interaction parameter within low-velocity limit. Numerous papers have been published on the studies of wake effects induced because of moving charge particle inside the medium. Spatial excitation patterns were studied by P.M. Echenique, R.H. Ritchie and Werner Brandt [88] which sets up two types of electron-density fluctuations, whereas A. Mazarro, P.M.Echenique and R.H.Ritchie [89] studied the charged-particle wake using the full random-phase approximation dielectric function of the medium. The Plasmon-pole approximation to the dielectric function gives a good account of most aspects of the wake when the velocity of the particle is greater than the Fermi velocity. The study of charged particle passing through Plasma has been made by Jacob Neufeld and R.

H. Ritchie [90]. Wake potential of swift ions in solids were computed using quantum-mechanical dielectric response function of the electron gas which includes Plasmon dispersion as well as single-particle effects at the densities of metallic conduction electrons. The effects of quantum fluctuations on the binding energy and the lifetime of the wake-riding state were also estimated by R.H.Ritchie, Werener Brandt and P.M. Echenique [91]. The study of energy loss by an external fast moving particle and wake effects are important physical phenomenon in physics which needs to be understood and studied for gapped graphene as it holds important place in device making replacing silicon based the semiconductors.

1.5 Collective excitations

Collective excitations arise due to interaction of many bodies. They are quanta associated with collective motions of the system as whole. Collective excitations have particle-like properties but don't resemble those of original particle of system. It helps to simplify the many-body phenomenon in terms of plasmons, phonons, magnons, Plasmon-phonon modes etc. to have a better understanding of the system. EELS (Electron energy loss Spectroscopy) and Light scattering experiments are the most useful tools to probe collective excitations. Theoretically useful information about collecctive excitations can be obtained by solving zeros of real part of eq. 1.13

$$Re\epsilon(\vec{q},\omega) = 1 - V_{\vec{q}}\chi_{01}(\vec{q},\omega) = 0 \qquad (1.19)$$

Where χ_{01} gives the real part of $\chi_0(\vec{q},\omega)$.

Extensive investigations, both theoretical as well as experimental, have been carried out on the collective excitations in carbon nanotubes, 2DEG and various superlattice structures. Because of realization of this artificial structure through various experimental techniques, it holds an important place in scientific and industrial application for its unique modified properties for developing high performance and high quality devices. Collective excitations include the magnons, plasmons, phonons, plasmon-phonon coupling etc. Plasmon dispersion relations for infinite periodic systems as well as for finite periodic systems for semiconductor superlattices was studied using self-consistent-field approach in detail by Das Sarma and J J Quinn [92]. The effect of uniform static external magnetic field oriented normal to the two-dimensional layers has also been included in addition with the use of hydrodynamic approximation. Coupled Plasmon-phonon modes (CPPM) for hetero-superlattices have been obtained by L.A. Falkovsky and E.G.Mishchenko [93]. Hetero-Superlattices consist of thin conducting planes separated by insulating layers. Reflectance of the sample has been obtained in infrared regions by evaluating phonon frequencies in the insulating layers. CPPM and their lineshapes for a doped semiconductor superlattice were studied in particular by Sharma A C and Sen R. They have implemented density-density correlation function to study the coupled modes [94]. Moreover the coupled modes were also reported in δ-doped polar semiconductors by Guo-Qiang Hai, Nelson Studart and Gilmar E. Marques [95]. RPA was used to study the coupling of collective excitations and their coupling to phonons. Their results indicate strong coupling at higher electron density. They have also published results for electron energy loss (eel) Interaction of collective excitations and LO-phonon mode of lattice for 2DEG is calculated within RPA by Wu Xiaoguang and F. M. Peeters and J. T. Devreese [96]. Discrete Plasmons were

observed by A. Pinczuk, M. G. Lamont and A.C. Gossard in layered 2DEG with finite number of periods. They have emphasized the importance of Raman light scattering experiments for observation of discrete plasmon doublets [97]. Plasmons for N equally spaced layers of two-dimensional electron gas within RPA is evaluated and Raman line shapes are predicted by Jainendra K. Jain and Philip B. Alien [98]. Collective excitations were obtained for modulation-doped GaAs/AlAs superlattice by Sharma A. C. and Sood A.K. [99]. The wavevector dependence were observed with the interaction of LO phonons and plasmons by L. F. Lemmens and J. T. Devreese in polaron gas [100]. Interaction of Plasmons and longitudinal phonons in a multilayer structure and superlattice by Caille and Bloss and Brody respectively [101,102].

Collective excitations in gapped graphene have been studied by Xue-Feng Wang and Tapash Chakraborty within Random Phase Approximation. The spin-orbit interaction opens up a gap between interband and intraband excitation continuum. The long-wavelength dielectric function changes drastically and an undoped plasmon mode appears in the electron-hole continuum gap reflecting the interplay between the intraband and interband electron correlations [103]. Plasmon bands were discussed by Kotov et.al. in their review article on graphene. These bands were obtained for infinite stacks of graphene layer [30]. Theoretical investigations on plasmons and the CPPM have been reported for SLG, within the diagrammatic self-consistent field theory. Two terahertz plasmon modes and four infrared CPPM can be achieved via intra-and inter-band transitions in graphene. Moreover it is noticed that with increasing $\boldsymbol{q}$ and carrier density, the plasma modes are strongly coupled with optic-phonon modes in graphene in the infrared region. [104] as well as for bilayer graphene [105]. A generalized theory for Plasmon studies was developed by

Das Sarma and E H Hwang for SLG and D-dimensional superlattice structure [106]. Excitation spectrum and high-energy plasmons in SLG and in multilayer graphene systems were studied by Yuan Shengjun *et.al.* and Horing N J M [77,107], while plasmonic excitations in Coulomb coupled N-layer balanced and unbalanced graphene structure was studied by J J Zhu et.al. at finite doping and temperatures [108]. Experimentally CPPM in Graphene nanoribbon (GNRs) and graphene nanoribbons arrays (GNRA) [109,110] have recently been investigated in view of applying graphene and graphene multilayer structures to plasmonic waveguides, modulators and detectors from sub-tetra hertz to mid-infrared regimes, and in obtaining efficient optoelectronic switching devices while, Liu and Wills [111] have reported the CPPM in epitaxial graphene, using angle-resolved reflection electron-energy-loss spectroscopy (AREELS). They have observed a transition from Plasmon like dispersion to phonon like dispersion when number of graphene layers is increased on SiC substrate.

1.6 Objective of thesis

Several experimental groups have reported interesting transport and spectroscopic measurements, which has led to rapidly burgeoning experimental and theoretical interest in this field. On the theoretical side, there has been a number of works in the literature on the effects of electron-electron interaction in graphene. However, explicit analytical results for either the doped or the undoped case were still lacking. The structure factor and pair correlation function, which gives important information about the excitation spectrum of the system, is studied using density-density response function within RPA. The exchange and correlation effects have been introduced using local field corrections (LFC) to obtain self energy,

screening charge density and screened potential. It is useful to investigate these ground state properties using simple methods.

With extensive research in SLG the introduction of gap is considered as a boon for experimentalists to see gapped graphene as a replacement for semiconductors in device application. Though many aspects have been investigated, the analytic support to few important numerical results were still missing. Wake effects have a large impact on the response of given system. These effects, created due to external charges, are important part of studies to be carried out as it helps to develop a model with optimum performance of a device with low energy loss and heat loss. The frequency dependence of the substrate and background dielectric constant, which would account for Plasmon-phonon coupling, has been investigated within RPA for GBS. Study of Plasmon-Phonon coupling paves way to experimentalists to verify and understand their results for the experiments done on Raman spectroscopy, EEL and inelastic light scattering. Moreover the theoretical study of superlattice can develop interest and curiosity to fabricate such system for further studies and refining of its properties so that these studies can have a better implication in device making technology. Theoretical studies on Plasmon-phonon coupling has been reported in this thesis.

1.7 References

1. H-S Philip Wong and Deji Akinwande Carbon Nanotube and Graphene Device Physics, Cambridge University Press, Ist Ed. (2011)

2. E.H.Hwang and S. Das Sarma Phys. Rev. B 75, 205418 (2007)

3. Jean-Christophe Charlier and Gian-Marco Rignanese, Phys. Rev. Lett. 86, 5970 (2001)

4. P. R. Wallace Phys. Rev. 71, 622 (1947)

5. S. Y. Zhou, G.-H. Gweon, J. Graf, A. V. Fedorov, C. D. Spataru, R. D. Diehl, Y. Kopelevich, D.-H. Lee, Steven G. Louie and A. Lanzara , Nat. Phys. 2, 595-599 (2006)

6. K. S. Novoselov Science 306, 666 (2004)

7. Wonbong Choi , Indranil Lahiri , Raghunandan Seelaboyina & Yong Soo Kang - Critical Reviews in Solid State and Materials Sciences, 35, 52–71, (2010)

8. Phaedon Avouris and Christos Dimitrakopoulos, Materials today, March 2012, vol 15 No. 3 86-97 (2012)

9. Jens Hofrichter Nano Lett. 10, 36-42 (2010)

10. Edward McCann and Mikito Koshino ***Rep. Prog. Phys.*** 76 056503 (2013)

11. R. Côté, Wenchen Luo, Branko Petrov, Yafis Barlas, and A. H. MacDonald Phys. Rev. B 82, 245307 (2010)

12. P.K. Pyatkovskiy Journal of Phys. Cond. Matt. 21, No.2 025506 (2009)

13. Alireza Qaiumzadeh and Reza Asgari Phys. Rev. B 79, 075414 (2009)

14. M S Dresselhaus Nano Lett, 10 No.3 ,pp 751-758 (2010)

15. Aaron Bostwick, Taisuke Ohta, Thomas Seyller, Karsten Horn and Eli Rotenberg - Nature Physics 3, 36 - 40 (2007)

16. Z. Q. Li, E. A. Henriksen, Z. Jiang, Z. Hao, M. C. Martin, P. Kim, H. L. Stormer and D. N. Basov1 - doi:10.1038/nphys989

17. Cheol-Hwan Park, Feliciano Giustino, Catalin D. Spataru, Marvin L. Cohen, and Steven G. Louie - Nano Letters 2009 Vol. 9 No. 12 4234-4239 (2009)

18. González, F. Guinea, and M. A. H. Vozmediano Phys. Rev. Lett. Vol. 77, No. 17, 3589

19. S. Das Sarma, E. H. Hwang, and Wang-Kong Tse - Phys. Rev. B 75, 121406 (R) 2007

20. E. H. Hwang, Ben Yu-Kuang Hu, and S. Das Sarma - Phys. Rev. B 76, 115434 (2007)

21. Marco Polini, Reza Asgari, Giovanni Borghi, Yafis Barlas, T. Pereg-Barnea, and A. H. MacDonald Phhys. Rev. B 77, 081411 (R) (2008)

22. R. Roldán, M. P. López-Sancho, and F. Guinea - Phys. Rev. B 77, 115410 (2008)

23. B. E. Sernelius EPL, 95, 57003 (2011)

24. Jalal Sarabadani, Ali Naji, Reza Asgari, and Rudolf Podgornik Phys. Rev. B 84, 155407 (2011)

25. Principi and Marco Polini G. Vignale M. I. Katsnelson, Phys. Rev. Lett. 104, 225503 (2010)

26. E. H. Hwang and S. Das Sarma - Phys. Rev. B 77, 081412 (R) (2008)

27. Bruno Uchoa, James P Reed, Yu Gan, Young II Joe, Eduardo Fradkin, Peter Abbamonte and Diego Casa, Phys. Scr. T 146 014014 (2012)

28. A.H. Castro Neto, F.Guinea, N.M.R. Peres, K.S. Novoselov and A.K.Geim Reviews of Modern Physics Vol 81 109-162, January-March 2009

29. S.Das.Sarma Shaffique Adam E.H.Hwang Enrico Rossi Reviews of Modern Physics,Vol 83, 407- 470, April-June 2011

30. Valeri N.Kotov, Bruno Uchoa, Vitor M. Pereira – Rev. Mod. Phys., Vol 84, 1067-1125, July-September 2012

31. D.S.L. Abergel, V.Apalkov, J. Berashevich, K. Ziegler and Tapash Chakraborty Advances in Physics Vol. 59 No. 4, 261-482, July – August 2010

32. Giuliani G F and Vignale G 2005 Quantum Theory of the Electron Liquid (Cambridge: Cambridge University Press)

33. B Wunsch ***et al New J. Phys.*** 8 318 (2006)

34. Rajdeep Sensarma, E. H. Hwang, and S. Das SarmaPhys. Rev. B 82, 195428 (2010)

35. G. Borghi, Marco Polini, Reza Asgari, and A. H. MacDonald Phys. Rev. B 80, 241402(R)

36. E.H.Hwang and S.Das.Sarma, Phys. Rev. Lett. 101 156802 (2008)

37. Jia-Ning Zhang Phys. Scr.83 035002 (2011)

38. Andreas Scholz, Tobias Stauber, and John Schliemann Dielectric Phys. Rev. B 86, 195424

39. A.Hill et al 2009 Euro. Phys. Lett. 87 27005

40. L.A. Falkovsky Journal of Physics: Conference Series 129 012004 (2008)

41. Tsuneya Ando Journal of the Phys. Soc. of Japan Vol. 75, No. 7, July, 2006, 074716

42. Yafis Barlas, T. Pereg-Barnea, Marco Polini, Reza Asgari, and A. H. MacDonald Phys. Rev. Lett 98, 236601 (2007)

43. J. Sabio, J. Nilsson, and A. H. Castro Neto Phys. Rev. B 78, 075410 (2008)

44. E. H. Hwang and S. Das Sarma Phys. Rev. B 79, 165404 (2009)

45. Saeed H. Abedinpour, G. Vignale, A. Principi, Marco Polini, Wang-Kong Tse, and A. H. MacDonald, Phys. Rev. B 84, 045429 (2011)

46. T.Stauber Phys. Rev. B 82, 201404(R)

47. S S Z Ashraf , A C Sharma and K N Vyas 2007 J. Phys.: Cond. Matter 19 306201 (2007)

48. Tanatar et.al. Phys. Rev. B 43 No.18 14621-14628

49. R. K. Moudgil and P. K. Ahluwalia K. Tankeshwar Phys. Rev. B 54 No.12, 8809-8813

50. Darren J.T. Leonard and Neil F. Johnson Phys. Rev. B 58 No. 23, 15 468-15482

51. B Tanatar and D.M. Ceperley Phys. Rev. B 39 No.8 5005-5016

52. Czachor, A. Holas, S. R. Sharma, and K. S. Singwi – Phys. Rev. B 25 No.4 2144-2159

53. F. Pederiva, E. Lipparini and K. Takayanagi Euro phys. Lett. ***40*** No. 6

54. G Barnea J. Phys. C : Solid State Phys.,Vol.12, L263-L268 (1979)

55. K. Shiyuza Phys. Rev. B 77, 075419

56. G D Mahan, Many Particle Physics IInd Ed. (Plenum, newYork, 1990)

57. Dharma Wardana Phys. Rev. B 75, 075427 2007)

58. D. S. L. Abergel and Tapash Chakraborty Phys. Rev. B 82, 161409 (R) (2010)

59. N. W. Ashcroft and N. D. Mermin, Solid State Physics, Saunders College, Philadelphia (1976)

60. Gabriele F. Giuliani, George E. Simion Solid State Comm. 127 789-791 (2003)

61. Masanori Ono, Takahiro Nishio, Toshu An, Toyoaki Eguchi, Yukio Hasegawa Appl. Sur. Sci. 256 469-474 (2009)

62. Vadim V. Cheianov and Vladimir I.Fal'ko Phys. Rev. Lett. 97 226801 (2006)

63. Ivan S. Terekhov, Alexander I. Milstein, Valeri N. Kotov, and Oleg P. Sushkov – Phys. Rev. Lett. 100, 076803 (2008)

64. Richard D. Mattuck, A guide to Feynman diagrams in the Many-Body problems, IInd Ed. Dover Publications, INC, New York

65. J.J. Quinn and Richard A. Ferrell Phys. Rev. Vol 112, No. 3, 812-827 (1958)

66. G C Aers and J B Pendry J. Phys.C : Solid State Phys. 15 3725-3732 (1982)

67. Yu. M. Malozovsky and S.M. Bose and P.Longe Phys. Rev B. 47, No. 22 15242- 15249

68. E. H. Hwang, Ben Yu-Kuang Hu, and S. Das Sarma Phys. Rev. B 76, 115434, (2007)

69. Andro Sabashvili, Stellan O. stlund, and Mats Granath - Phys. Rev. B 88, 085439 (2013)

70. J. Martin, N. Akerman, G. Ulbricht, T. Lohmann, J. H. Smet, K. Von klitzing and A. Yacoby - Nat.Phys. 4 144 (2008)

71. D.E. Sheehy and J. Schmalian Phys. Rev. Lett. 99 (2007) 226803

72. D.S.L. Abergel, P. Pietilainen and T. Chakraborty Phys. Rev. B 80 081408 (R) (2009)

73. E. A. Henriksen and J. P. Eisenstein - Phys. Rev. B 82 041412(R)

74. Qiuzi Li, E. H. Hwang, and S. Das Sarma Phys. Rev. B 84 235407

75. F. Young, C. R. Dean, I. Meric, S. Sorgenfrei, H. Ren, K. Watanabe, T. Taniguchi, J. Hone, K. L. Shepard, and P. Kim Phys. Rev. B 85, 235458

76. N.H. March and M. Parrinelo, Collective effects in solids and liquids, Adam Hilger Ltd. Bristol, University of Sussex press

77. Horing N J M Phil. Trans. R. soc. A 368, 5525-5556 (2010)

78. Vassilios fessatidis Phys. lett. A 375 192-198 (2010)

79. Godfrey Gumbs Journal of Mod. Opt. 58 No. 21, 1990-1996 (2011)

80. I Radovic, L.J. Hadzievski and Z L Miskovic Phys. Rev. B 77 075428 (2008)

81. A.Bergara, J.M. Pitarke and P. M. Echenique Phys. Rev. B 59 No 15 10145

82. A.Bergara, I.Nagy and P.M.Echenique. Phys. Rev. B 55 No. 19 12864

83. R Nunez, P.M. Echenique and R.H.Ritchie J. Phys. C : Solid St. Phys. 13 4229-46 (1980)

84. Chun-Zhi Li, Yuan-Hong Song, You-Nian Wang Phys. Lett. A 372 4500-4504 (2008)

85. Radovic,V Borka Jovanovic, D. Borka, Z. L. Miskovic Physics Research B 279 165-168 (2012)

86. Ivan Radovi, Duško Borkaa, Zoran L. Miškovi Physics Letters A 375 3720–3725 (2011)

87. You-Nain Wang and Teng-Caj Ma Phys. Rev. B 52,No. 23 16395- 16399

88. P.M. Echenique, R.H. Ritchie and Werner Brandt Phys. Rev. B 20 No. 7 2567-2580

89. AMazarro, P.M.Echenique and R.H.Ritchie Phys. Rev. B 27 No. 7 4117-4128

90. Jacob Neufeld and R. H. Ritchie Phys. Rev. B 98 No.6 1632-1642

91. R.H.Ritchie, Werener Brandt and P.M. Echenique Phys. Rev. B 14 No.11 4808-4812

92. S Das Sarma and J J Quinn Phys. Rev. B 25 No. 12 7603 (1982).

93. L.A. Falkovsky and E.G.Mishchenko JETP Letters, 82, No. 2, 96-100 (2005).

94. A C Sharma and R Sen J. Phys Cond Matter 7 9551-9561 (1995)

95. Guo-Qiang Hai, Nelson Studart and Gilmar E. Marques Phys. Rev. B 55 No.3 1554-1562 (1997)

96. Wu Xiaoguang and F. M. Peeters and J. T. Devreese Phys. Rev. B 32 No. 10 6982

97. A. Pinczuk, M. G. Lamont and A.C. Gossard Phys. Rev. B 56 No. 19 2092 (1986)

98. Jainendra K. Jain and Philip B. Alien Phys. Rev. B 54 No. 22 2437

99. A. C. Sharma and A.K. Sood J. Phys. Cond matter 6 1553-1562 (1994).

100. L. F. Lemmens and J. T. Devreese Solid State Comm 14 1339-1341, (1974)

101. A. Caille, M. Bonville and M.J. Zukermann Solid State Comm. Vol. 24 pp 805-808, (1977)

102. W. L. Bloss and E.M. Brody Solid State Comm. 43, No.7, pp 523-528 (1982)

103. Xue-Feng Wang and Tapash Chakraborty - Phys. Rev. B 75, 033408 (2007)

104. Dong H M, Li L L, Wang W Y, Zhang S H, Zhao C X, Xu W Physica E 44 1889–1893 (2012)

105. Hwang E H, SenSarma Rajdeep, and Sarma S D Phys Rev B 82, 195406 (2010)

106. SarmaS D, Hwang E H Phys Rev Lett 102,206412 (2009).

107. Yuan Shengjun, Roldan R, and Katsnelson M I. Phys Rev B 84, 035439 (2011)

108. Zhu J J, Badalyan S M, and Peeters F M Phys. Rev. B 87, 085401 (2013)

109. Freitag arXiv 1306.0593v1

110. Hugen Yan arXiv 1209.1984v1

111. Liu Yu, Wills R F Phys. Rev. B 81, 081406(R) (2010)